Journal of Advanced Zoology
ISSN: 0253-7214
Volume 43 Issue S2 Year 2022 Page 36-47

Formulation And Characterization of Chitosan Nanoparticle Loaded Gamma Oryganol for Antioxidant Activity

Rathore G S[1*], Chauhan C S[2]

[1*]*School of Pharmacy, MVSC Janardhan Rai Nagar Rajasthan Vidyapith, Udaipur, gajendrasrathore89@gmail.com*
[2]*Bhupal Nobal's Institute of Pharmaceutical Sciences, Bhupal Nobal's University, Udaipur*
Email: neerajsharma236@gmail.com

Abstract

The present study focuses on the formulation, characterization, and evaluation of chitosan nanoparticles loaded with gamma oryzanol (CG nanoparticles) aimed at enhancing its antioxidant and therapeutic efficacy. Nanoparticles were synthesized via a solvent evaporation technique using varying ratios of chitosan and drug. The prepared formulations were assessed for percentage yield, drug entrapment efficiency (EE), particle size, polydispersity index (PDI), and morphological characteristics. The % yield ranged between 81.45–98.12%, while EE varied from 68.34±3.15% to 94.15±1.24%. Particle size analysis showed nanometric sizes between 710.02±1.20 nm to 904.25±1.12 nm, with PDI values indicating acceptable uniformity for pulmonary delivery. SEM imaging confirmed spherical, moderately agglomerated nanoparticles, and DSC and FTIR analyses indicated significant drug-polymer interaction and amorphous nature of the encapsulated drug. In vitro drug release studies demonstrated sustained release behavior over 24 hours, with CG5 showing the highest cumulative release. Antioxidant potential evaluated via DPPH, ABTS, and FRAP assays confirmed significant free radical scavenging capacity. These findings suggest that CG nanoparticles could be a promising carrier for gamma oryzanol with enhanced stability, bioavailability, and therapeutic activity.

Keywords: Chitosan nanoparticles, gamma oryzanol, ionic gelation, antioxidant activity, sustained release, streptozotocin.

Introduction

Diabetes mellitus is one of the most prevalent and challenging chronic metabolic disorders worldwide. It is characterized by persistent hyperglycemia resulting from impaired insulin secretion, insulin action, or both. The condition affects carbohydrate, fat, and protein metabolism and, if left untreated, can lead to severe complications such as retinopathy, nephropathy, neuropathy, cardiovascular diseases, and poor wound healing (Rawal *et al.*, 2018; Panday *et al.*, 2023). According to the International Diabetes Federation (IDF), over 537 million adults were living with diabetes in 2021, and the number is expected to rise to 783 million by 2045. This alarming trend underscores the urgent need for effective, safe, and affordable therapeutic strategies for diabetes management (Elmowafy *et al.*, 2023; Khormali).

Although various synthetic oral hypoglycemic agents and insulin therapies are available, they are often associated with several limitations, including side effects, high cost, and poor patient compliance. Consequently, attention has shifted toward exploring alternative approaches, particularly those based on natural products and phytochemicals that offer potential therapeutic benefits with minimal adverse effects (Choudhary *et al.*, 2023).

Gamma oryzanol (γ-oryzanol) is a naturally occurring mixture of ferulic acid esters of phytosterols and triterpene alcohols, predominantly found in rice bran oil. It exhibits a wide range of pharmacological properties, including antioxidant, anti-inflammatory, lipid-lowering, and neuroprotective effects. Recent studies have also demonstrated its potential role in improving glucose metabolism and insulin sensitivity, suggesting its utility as a promising therapeutic agent for managing diabetes mellitus (Dewanjee *et al.*, 2020). However, the clinical application of gamma oryzanol is significantly limited due to its poor aqueous solubility, low gastrointestinal absorption, and rapid metabolic degradation, which collectively result in low systemic bioavailability. To overcome these challenges, novel drug delivery systems are required that can enhance the solubility, stability, and targeted delivery of gamma oryzanol (Sharif *et al.*, 2022).

Nanotechnology-based delivery systems have emerged as a powerful tool to address the limitations associated with conventional dosage forms. Among them, polymeric nanoparticles have gained considerable attention for the delivery of poorly soluble drugs. Chitosan, a natural polysaccharide obtained by the deacetylation of chitin, is extensively used in pharmaceutical applications due to its favorable characteristics, including biocompatibility, biodegradability, mucoadhesiveness, and ability to transiently open tight junctions in epithelial cells, thus facilitating enhanced drug absorption across biological membranes (Nie *et al.*, 2020; Paul *et al.*, 2021).

Chitosan nanoparticles can be easily prepared via the ionic gelation method, which involves the electrostatic interaction between the positively charged amino groups of chitosan and negatively charged crosslinkers like sodium tripolyphosphate (TPP). This technique is advantageous due to its simplicity, mild preparation conditions, and avoidance of harsh organic solvents or high energy input (Rana & Bala, 2024; Bera *et al.*, 2023).

In this study, we aim to develop chitosan-based nanoparticles encapsulating gamma oryzanol to improve its solubility, protect it from premature degradation, and achieve controlled release for prolonged therapeutic action. The formulated nanoparticles will be extensively characterized for their physicochemical properties, including particle size, zeta potential, encapsulation efficiency, and drug release behavior. Furthermore, the antidiabetic potential of the gamma oryzanol-loaded chitosan nanoparticles will be evaluated in streptozotocin (STZ)-induced diabetic rat models, assessing their efficacy in reducing blood glucose levels and improving pancreatic histology.

This approach not only aims to harness the natural therapeutic potential of gamma oryzanol but also demonstrates the capability of chitosan-based nanocarriers to enhance the delivery and efficacy of phytochemicals in the treatment of chronic metabolic disorders like diabetes mellitus.

Materials and Methods

Materials

High molecular weight chitosan (MW: 350,000 g/mol, deacetylation degree >75%, and viscosity 800–2000 cps), sodium tripolyphosphate (TPP), and ferric ammonium citrate were procured from Sigma-Aldrich Co (St. Louis, MO, USA). Gamma Oryzanol was obtained from India Mart. All additional materials and solvents employed in this research were of analytical grade.

Methods

Preparation of Chitosan Nanoparticle loaded with Gamma Oryzanol (CG Nanoparticle)

We made CG nanoparticles using a method called ionotropic gelation (Yang & Chiang, 2019). To create blank nanoparticles, we added a TPP aqueous solution (final concentration 1 mg/mL) to a CG acetic acid solution. The CG/TPP ratio was 2/1 (weight/weight), and we used different stirring rates (400, 800, and 1200 rpm). For drug-loaded nanoparticles, we gamma oryganol (GO) aqueous solutions with CG, and TPP was added slowly to form the nanoparticles. Each sample was prepared three times, and the results are the average. We removed any non-entrapped drug and dissolved CG by ultra-centrifugation at 13,000 rpm for 20 minutes and then reconstituted from the precipitate in fresh water (twice). The resulting suspension was frozen and lyophilized using a freeze-drier system (Scanvac, Coolsafe 110-4 Pro, Labogen Scandinavia) for 24 hours at −108 °C to get a dried nanoparticle product (Table 1).

Table 1: Preparation of Chitosan Nanoparticles loaded with Gamma Oryzanol

Formulation Code	Gamma Oryzanol (mg/ml)	Chitosan (mg/ml)	Tripolyphosphate (mg/ml)	Acetic Acid (mg/ml)
CG 1	2	5	1.25	0.8
CG 2	1	2	2	0.5
CG 3	2	3.5	1.25	0.5
CG 4	1.5	2	1.25	0.2
CG 5	1.5	2	1.25	0.8
CG 6	1	3.5	2	0.8
CG 7	1.5	3.5	2	0.2
CG 8	2	5	0.5	0.5
CG 9	1.5	3.5	0.5	0.8
CG 10	1	3.5	0.5	0.2
CG 11	2	5	2	0.5
CG 12	1	5	1.25	0.2

Evaluation Parameters

Percentage yield

In this study, the theoretical yield was determined by calculating the maximum amount of the product that could be formed based on stoichiometry. The actual yield, representing the quantity of product obtained from the experimental procedure, was then calculated. The percentage yield, a key metric in assessing the efficiency of a reaction, was determined by expressing the actual yield as a percentage of the theoretical yield. This parameter provides valuable insights into the effectiveness of the reaction process, highlighting any potential inefficiencies or losses. The review article likely discusses the importance of percentage yield in evaluating the success of chemical reactions, emphasizing its role in quantifying the practical outcome compared to the theoretically predicted yield (Bairagee *et al.*, 2022).(Table 2)

$$\%Yield = \frac{\text{Actual yield}}{Theoritical\ yield} X\ 100$$

Table 2: Property Showing %Yield

% Yield with Property
Quantitative if % yield is around 100
Excellent if % yield is > 90
Very good if % yield is > 80
Good if % yield is > 70
Fair if % yield is > 50
Poor if % yied is < 40

Drug Entrapment Efficiency (%EE)

The process of ultracentrifugation was employed to distinguish the free drug from gamma oryzanol loaded chitosan nanoparticles (CG), which served as carriers for encapsulating the drugs in nanoparticle form. The centrifugation was carried out at speeds of up to 18,000 rpm for a duration of 40 minutes. Following the centrifugation, the supernatant liquid, containing any free drug that was not encapsulated within the nanoparticles, was carefully collected. Subsequently, this collected supernatant from CG underwent analysis for the concentration of GO. The analysis was conducted using UV Spectroscopy at specific wavelengths, namely 315 nm for GO. This analytical approach allowed for the quantification of the free drug concentrations in the samples, providing insights into the encapsulation efficiency and drug-loading capacity of the chitosan nanoparticles.

$$\%EE = \frac{(\mathrm{Dt} - \mathrm{Ds})}{(Da)} X\ 100$$

Dt= Drug incorporated in the formulation, Ds = Concentration of the drug in the supernatant liquid

Particle size and Poly Dispersity Index

The particle size and PDI (Polydispersity Index) of CG were determined using the Malvern Zeta Sizer Nano (ZS90). This involved diluting the samples with deionized water. The characteristics related to dispersion quality, stability, and particle size of CG were assessed using dynamic light scattering at an angle of 90 degrees.

This process was repeated three times (n=3) to ensure reliability and consistency of the measurements. The analyses were conducted at a temperature of 25°C. The obtained data provided insights into the physical properties of the nanoparticles, which are crucial for their characterization and potential applications in various fields (Bairagee et al., 2024).

Scanning Electron Microscopy (SEM)

The shape and texture of the particles were analyzed using a Hitachi S-4300 microscope. For sample preparation, an Emscope SC400 sputter coating system was employed to coat the samples with a thin film of gold/palladium. This coating was applied to samples previously positioned on adhesive carbon tabs attached to aluminum stubs. Maintaining a working distance of 13.3 mm, an electronic beam was directed at the coated samples at an accelerating voltage of 8-10 kV. Consistent conditions were applied to capture images at various magnifications, providing detailed insights into the morphology and structure of the particles. This analytical approach was crucial for understanding the physical characteristics of the particles under investigation (Bairagee *et al*., 2019).

Differntial Scanning Colorimetery (DSC) of optimized formulation

To ensure uniform temperature distribution within the sample, a thin layer was evenly spread to establish optimal contact with the base. Employing a small sample size (< 5 mg) facilitated rapid heat flow through the pan. The heating rate was configured at 50°C/min across a temperature range of 50-400°C, enhancing the signal-to-noise ratio for precise analysis (Tiruwa, 2016).

FT-IR of Optimized formulation of CG

To validate the occurrence of ionic gelation between the amine group in chitosan and the phosphate group in tripolyphosphate, Perkin Elmer Spotlight 200i FT-IR was employed. The scanning range spanned approximately 4000-400 cm^{-1}. Dried CG were uniformly taken and compressed into KBr pellets using a round flat-faced punch, ensuring the samples were prepared for scanning (Date *et al.*, 2016).

In-Vitro Drug Release of CG Nanaoparticles

In-vitro dissolution studies for the optimized CG nanoparticles were conducted through the dialysis bag method. Phosphate buffer at pH 7.4 (250 ml) and simulated colonic fluids for both fed and fasted states (250 ml each) served as the dissolution media. Prior to the experiment, the dialysis bags (2000 Da) were soaked overnight in deionized water. Subsequently, 2 ml of the optimized nanoparticle dispersion was transferred to the dialysis bag, clamped at both ends. The dissolution fluid was maintained at a temperature of 35±0.5°C, and drug release was monitored over 24 hours. Samples were withdrawn at specified intervals (1 ml each time), ensuring sink conditions by adding an equal volume of fresh dissolution fluid. Analysis of the samples for sulfasalazine and methylprednisolone was performed at 359 nm and 242 nm, respectively, using a UV Spectrophotometer. All measurements were conducted in triplicate (Bairagee *et al*., 2022).

Antioxidant Activity

Energy for biological activities is produced via oxidation, which is necessary for many living things. Yet, an excess of O2-centered permitted radicals and reactive O2 species can harm or even kill living organisms through cellular damage. Therefore, understanding the role of reactive oxygen species and free radical reactions in biological systems is of great interest at the moment. Superoxide anions, hydroxyl radicals, and hydrogen peroxide are produced in significant quantities when there is an excess of oxygen or insufficient reduction. Among the various defensive mechanisms mammalian cells have to stave against harmful effects are metabolic systems like glutathione peroxidase, catalase, and superoxide dismutase. Antioxidant defences in the body involve not just antioxidant enzymes but also nonenzymatic substances including thioredoxin, thiols, and disulfide-bonding (Antolovich *et al.*, 2002).

A vital part of the antioxidant defence system are also exogenous substances like zinc and selenium and micronutrients like β-tocopherol, β-carotene, and ascorbic acid. Severe oxidative damage to a variety of macromolecules can happen, though, if the body's natural antioxidant defences aren't able to eliminate radical species entirely. Mutations in DNA, lipid peroxidation of the membranes, and decreased membrane fluidity can all result from radical species' substantial oxidative damage to DNA and cell membranes. Ageing and the onset of illnesses including diabetes, cancer, cirrhosis, arteriosclerosis, and other degenerative diseases have been linked to these harmful impacts.

By functioning as reducing agents, complexers of pro-oxidant metals, scavengers of free radicals, and quenchers of singlet oxygen generation, antioxidants have shown their value in the prevention of illness. There are several artificial antioxidants that are frequently included in processed foods that have been shown to have negative side effects, including ascorbic acid, butylated hydroxytoluene, and butylated hydroxyanisole. Additionally, it has been proposed that there may be a negative correlation between the frequency of specific human diseases and the use of foods high in antioxidants. In the last few years, a wide range of aromatic herbs and spices have been studied for their antioxidant qualities. As a result, more and more medications and formulations based on antioxidants are being developed for the treatment and prevention of complex illnesses like cancer, diabetes, Alzheimer's disease, cardiovascular disease, and stroke. Many plants have yet not been well investigated, though, or our understanding of their antioxidant potential is still lacking. Therefore, more study is needed to determine the natural sources of antioxidants. The usage of diverse approaches to assess the antioxidant efficiency of these chemicals is increasing in tandem with the growing significance of this study. We used a number of standard procedures in our study that were readily adaptable to our lab environments.

DPPH radial scavenging activity

In order to assess anti-oxidant action, the DPPH method has become increasingly popular in recent years. Due to the spare electron's delocalization over the whole molecule, the DPPH radical is stable unlike most other free radicals, which often dimerize. With a notable absorption maximum at 517 nm, this radical has a pronounced purple colour. The DPPH radical changes from purple to yellow when it interacts with an antioxidant that scavenges free radicals, allowing the odd electron to connect with hydrogen and create reduced DPPH-H. Molar absorptivity at 517 nm decreases as a result of this reaction, going from 9660 to 1640. Marsden Blois developed the DPPH method more than 50 years ago, and it works with both liquid and solid materials. Instead than focusing on any one antioxidant component in particular, it assesses the sample's overall antioxidant potential (Shahidi & Zhong, 2015) (Figure 1).

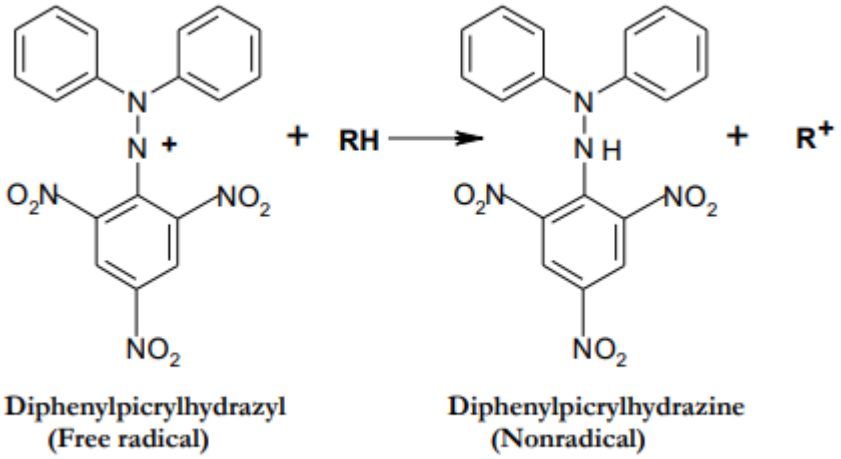

Figure 1: DPPH Radical

Assay Procedure

The interaction between antioxidants and DPPH, a steady free radical that transforms into DPPH-2H upon reduction, leads to a reduction in absorbance as the DPPH radical changes to the DPPH-H form. The extent of discoloration serves as an indicator of the capacity of antioxidant compounds or extracts to donate and scavenge hydrogen. The capacity of the ethanolic extract of A. aspera leaves to scavenge free radicals (DPPH) was examined in accordance with Blois's methodology (15). We combined recently prepared DPPH solution (0.004% w/v) in 99% methanol with 100µg/ml of methanol sample solutions. Following a 20-minute incubation at RM in darkness, the absorbance of the combination was slow at 517 nm by means of a spectrophotometer. Elliott's acid served as the orientation normal. A control sample, with the same volume but lacking any extract, was prepared, and the blank consisted of 99% methanol. A decrease in absorbance of the response combination designated larger free radical scavenging movement. The DPPH free fundamental scavenging percentage was calculated for each test, conducted in duplicate, utilizing the subsequent calculation:

DPPH radical scavenging activity (%) = ($A_{control}$ - A_{test})/$A_{control}$ X 100.

Assuming that A_{test} is the absorbance in the company of the extracts or standard, and $A_{control}$ is the absorbance of the control reaction.

Superoxide scavenging activity

In the superoxide scavenging mechanism, NBT reduction is crucial. Nitroblue tetrazolium (NBT) in this instance is converted to NBT diformazan by the superoxide radical. NBT is reduced to a purple formazan by superoxide radicals, which are created when the phenazine methosulfate-nicotinamide adenine dinucleotide (PMS-NADH) complex oxidises NADH. When nitroblue tetrazolium was photochemically reduced, it was discovered that the extracts from Achyranthes aspera and Phaseolus vulgaris Linn. demonstrated superoxide radical scavenging ability by inhibiting the production of formazan (NBT). It is evident from these extracts' decreased absorbance at 560 nm that superoxide radicals in the reaction mixture can be attenuated (Moharram & Youssef, 2014).

Assay Procedure

With alkaline dimethyl sulfoxide (DMSO), superoxide scavenging activity was carried out. Prior to use, the solution that resulted from the reaction of solid potassium superoxide and dry DMSO was filtered after at least 24 hours. It was decided to combine 200 ml of the previously indicated filtrate (56 mM) with 2.8 ml of an aqueous solution containing nitroblue tetrazolium. 1 ml of potassium phosphate buffer and 10 mM EDTA were added to this mixture in each test tube (10 mM, pH 7.4). Next came the introduction of 1 millilitre of extract that was varied in concentration (50–250 g/ml). When pure DMSO was used in place of alkaline DMSO as a control, the absorbance at 560 nm was determined.

Effect of scavenging (%) = [(1-AS/AO) X100]
Where, AO = Absorbance of control, AS = Absorbance of Sample

Nitric oxide scavenging activity

The test for scavenging free radicals in nitric oxide requires the diazotization procedure. Here, the interaction between oxygen and sodium nitroprusside yields NO, which in turn creates nitric ions.
The techniques of Sreejayan and Rao (1997) and Jagetia et al. (2004) were applied in order to quantify the nitric oxide scavenging capability of mushroom extract.

Assay Procedure

The nanoparticles was reconstituted in ethanol to achieve a con. of 10 mg/ml. Subsequently, the extract underwent several dilutions with distilled water to obtain con. from 50 to 250 µg/ml. The treated samples were then stored in a freezer at 4°C for future use.
In phosphate buffered saline, 0.5 millilitres of 10 mM sodium nitroprusside and one millilitre of extract were mixed at various dosages ranging from 50 to 250 µg/ml. The mixture was then incubated at 25°C for 180 minutes.
Just prior to use, the Griess reagent was made by mixing equal parts of 0.1 percent naphthylethylene diamine dihydrochloride, 2.5 percent phosphoric acid, and 1 percent sulphanilamide. After the three hours of incubation, the extract was varied with an equivalent volume of newly made Griess reagent. The same volume of buffer was added to a control sample, which was made without extract. A 546 nm absorbance measurement was made. The positive control in this experiment was gallic acid. The standard and extract's % inhibition was computed and noted. To calculate the percentage of nitric oxide radical scavenging activity of the gallic acid and ethanolic extracts, the following formula was used: Nitric oxide scavenged % = $A_{control} - A_{rest}/A_{control}$ X 100
Here A control = absorbance of control sample and A test = absorbance in the presence of extracts or standards (Jagetia & Lalhmangaihi, 2018).

Metal Ion chelating activity

Numerous biological activities can take place as a result of the ferrous ion's ability to transmit electrons. When iron chelators and tissue iron mix, stable, soluble complexes are created that are then eliminated in the urine or faeces.

Assay Procedure

We assessed the ferrous ion-chelating capacities of CG. FeCl2 (4H2O) (2 mM) solution was combined with one millilitre of CG at different doses (50–250 µg/ml). Five minutes were given to the response combination to incubate at RM. Following incubation, the response was introduced by addition of zero point one milliL of ferrozine (5 mM). Subsequently, 3 cc of DW was added to fill the container, and the mixture was thoroughly shaken before being allowable to stand for 10 minutes at RM. The absorbance of the solution was measured at 562 nm. The formation of the ferrozine-Fe2+ complex was quantified as a percentage of inhibition by means of the provided formula.

Metal chelating effect (%) = [A0-A1/A0] X 100
Here A control = absorbance of control sample and A test = absorbance in the presence of extracts or standards.

In vitro enzyme inhibitory activity

The medicinal plant has antidiabetic qualities because of its strong phytoconstituent composition. The secondary metabolites in the plant have the ability to increase the release of insulin in addition to improving glucose transport and metabolism in muscles. The action of natural products on carbohydrate-binding sites is thought to be the mechanism. The key to this process is the well-known debranching capacity of the enzymes α-glucosidase and α-amylase. Before being absorbed, these enzymes hydrolyze dietary polysaccharides into disaccharides and monosaccharides. Bioactive substances like flavonoids and polyphenols inhibit these enzymes, delaying the digestion and absorption of carbs and so reducing postprandial glucose levels.

α-glucosidase enzyme inhibitory activity

Assay Procedure

The assessment of the α-glucosidase enzyme's inhibitory activity involved monitoring the release of 4-nitrophenol from p-nitrophenyl-D-glucopyranoside. A mixture of 3.3 milliliters of 10 mM p-nitrophenyl α-D-glucopyranoside, 0.1 milliliters of potassium phosphate (pH 6.8), and the enzyme α-glucosidase was prepared. Acarbose, LE, and ODE solutions at various concentrations (0.2 ml) were added to the mixture as supplements. In every test tube, there was 1.7 cc of liquids (Ghannam *et al.*, 1986).

Following the incubation at 37°C for 30 minutes, the reaction mixtures were stopped by adding 2.0 ml of 100 mM sodium carbonate. The measurement of the released p-nitrophenol was conducted at 400 nm using a spectrophotometer. The % inhibition rates were then calculated using the formula below:

- $\%Inhibition = Abs_{control} - Abs_{sample} / Abs_{control} \times 100$

Results and Discussion

Preparation of Chitosan Nanoparticle loaded with Gamma Oryzanol (CG Nanoparticle)

The prepared chitosan nanoparticles loaded with gamma oryzanol was given in figure 2.

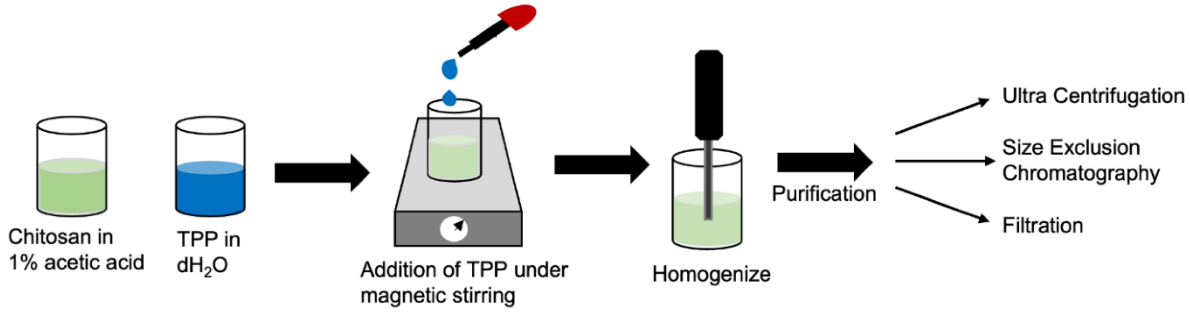

Figure 2: Preparation of chitosan nanoparticles laoded with gamma oryzanol

Evaluation of CG Nanoparticles

Percentage Yield

The % yield of chitosan nanoparticles was found to be in the range of 81.45 to 98.12% for all prepared batches shown in Table 7.1. Drug particles were wasted less, the gamma oryzanol is insoluble in water and the drug entrapment increases. That increases the nanoparticles to 98.12%. The sonication time directly affects the %

yield due to the drug was less solubilize under sonication and the % output of nanoparticles is increased with % yield.

Drug Entrapment Efficacy

The drug entrapment efficiency of nanoparticles containing drug: polymer in various ratios of was found to be 68.34±3.15 to 94.15±1.24% respectively (Table 3). As a result, increasing the polymer content in the formulation resulted in a continuous increase in entrapment efficiency. The high entrapment efficiency is likely due to electrostatic interactions between the drug and the polymer.

Table 3: Drug entrapment efficacy

Batch	Drug (mg)	CS (mg)	% Yield	%EE	MPS (nm)	PDI
CG 1	2	5	98.12	94.15±1.24	904.25±1.12	0.494±0.012
CG 2	1	2	81.45	77.07±2.04	761.23±1.23	0.344±0.002
CG 3	2	3.5	85.12	81.23±1.13	806.12±1.45	0.364±0.018
CG 4	1.5	2	82.23	78.23±2.08	765.23±1.21	0.314±0.013
CG 5	1.5	2	83.05	79.12±1.04	782.12±1.15	0.324±0.019
CG 6	1	3.5	84.09	80.23±3.04	802.15±1.34	0.394±0.022
CG 7	1.5	3.5	91.05	84.12±2.05	812.23±1.26	0.414±0.045
CG 8	2	5	90.23	70.34±2.34	719.45±1.18	0.312±0.024
CG 9	1.5	3.5	88.23	71.23±1.56	712.08±1.19	0.344±0.078
CG 10	1	3.5	87.03	68.34±3.15	710.02±1.20	0.304±0.013
CG 11	2	5	94.45	69.45±3.38	722.23±1.45	0.309±0.043
CG 12	1	5	92.23	78.32±2.76	773.12±1.67	0.456±0.061

Mean particle size (MPS nm), Polydispersity index (PDI), % Drug entrapment efficiency (%EE), Percentage yield (% yield)

Particle size and Poly Dispersity Index

The spherical particles were formed of gamma oryganol nanoparticles by using low molecular weight chitosan with solvent evaporation method of preparation. The particle size is affected by the incorporation of the organic solvent containing GO into chitosan solution with polyvinyl alcohol under a magnetic stirrer. The mean particle size ranged from 710.02±1.20 nm to 904.25±1.12 nm as seen in Table 3. Particle size was highly influenced by chitosan concentration and molecular weight (medium and high molecular weight). Higher chitosan concentration produced larger nanoparticles due to larger droplet size formation during emulsification. F2 formulation (50 mg chitosan) had the smallest particle size as compared to the F7 formulation (300 mg).

Nanoparticles with PDI smaller than 0.4 has to considered acceptable for drug delivery of nanoparticles to a deep pulmonary region (alveoli) according to some references. The term “polydispersity” is used to describe the degree of non-uniformity of size distribution of particles. The PDI of pirfenidone nanoparticles by solvent evaporation method was found to be 0.304±0.013 to 0.494±0.012 range (Table 3). As the PDI value increases, the heterogeneity in cross-linking, network formation, chain length, branching, and hyper branching will be more with more random arrangement.

SEM

The surface morphological structure was further examined by SEM analysis. SEM images of optimized formulation showed that the nanoparticles were spherical in shape and particles in the agglomerated state (Figure 3). Furthermore, the size uniformity of the nanoparticles is shown. Most of the particle size was found to be 501.9 ± 16.8 nm, which is suitable for the inhalation formulation. The particle size of a PFD formulation intended for inhalation, together with the particle density, is an important factor in the formulation's effectiveness since it affects the powder's dispersion and sedimentation properties. The rest of the cases aggregation occurred due to moisture entrapment during handling.

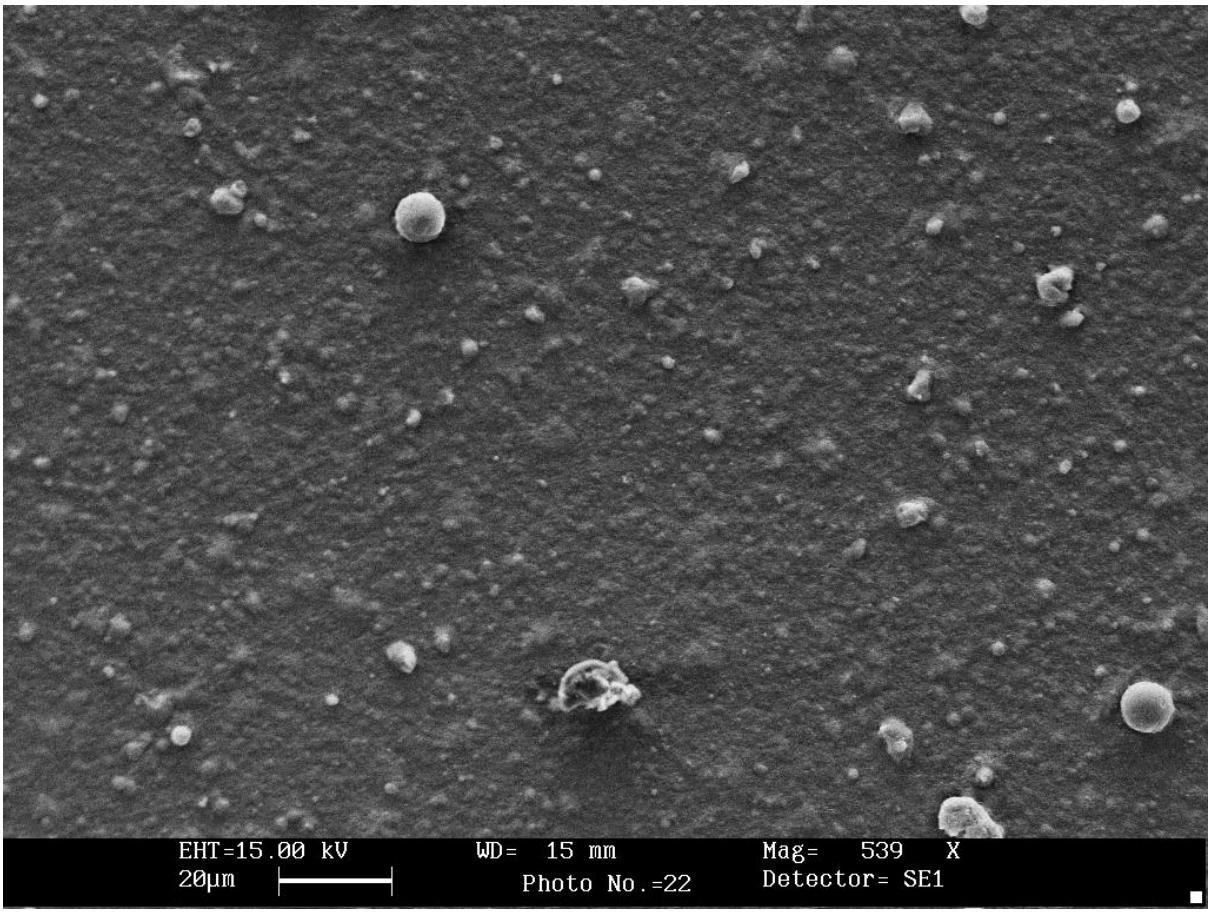

Figure 3: SEM image of CG nanoparticle

DSC

Figure 4 depicts the DSC thermogram of a drug-loaded niosomal formulation (F5). Endotherms were observed at 167.142°C (area=55.412 mJ, delta H=18.471 J/g) and 176.190°C (area=54.198 mJ, delta H=18.066 J/g). Endotherm at 176.190°C corresponds to surfactant thermal decomposition (span 60), whereas endotherm at 167.142°C indicates an increase in niosome phase transition temperature after drug loading. CG lack of a melting endotherm suggested that the drug had transitioned from crystalline to amorphous. These findings point to a significant interaction of the drug with the bilayer structure, which may account for improved drug entrapment in niosomal formulations and sustained drug release.

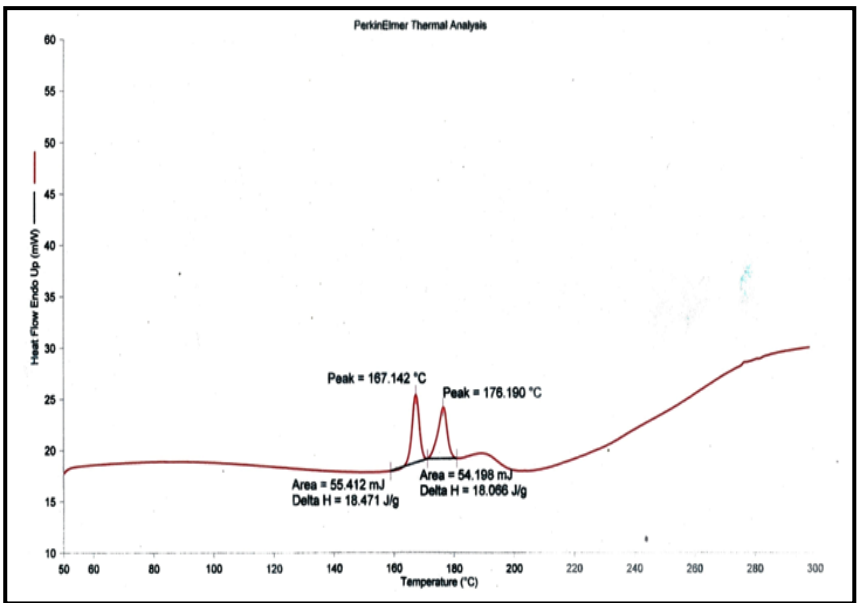

Figure 4: DSC thermogram tracings of drug loaded Nanoparticles.

FT-IR

The FT-IR spectra of optimized gamma oryganol loaded chitosan nanoparticles is given in figure 5 and table 4.

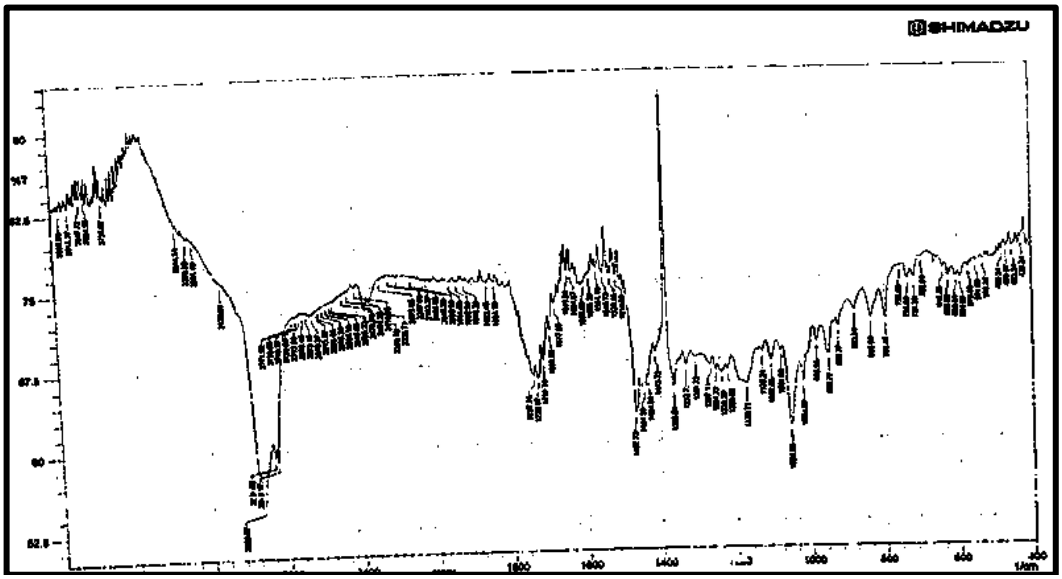

Figure 5: FTIR spectra of optimized formulation

Table 4: Interpretation of FTIR spectra of optimized formulation

S. No.	Functional group	Reported frequency (cm^{-1})	Observed frequency (cm^{-1})
1	N-H stretching	3400-3250	3217.10
2	N-H bending	1650-1580	1540.13
3	N-H wagging	910-665	632.26
4	C=N stretching	1700-1600	1677.95
5	C-H stretching	3000-2850	2937.38
6	C-H bending	1470-1450	1427.23
7	Aromatic C=C stretching	1675-1650	1637.45
8	O-H stretching, H-bonded	3500-3200	3400.27
9	C-O-C stretching in ring	1150-1000	1116.71

Drug Relaease

The percentage of drug released from the prepared nanoparticles in PBS pH 7.4 after 8 hours ranged from 79.23±1.12% to 92.45±1.64%. (Figure 5). It has been discovered that nanoparticle formulations can be released after 24 hours in the following decreasing order:

CG5>CG3>CG4>CG6>CG10>CG8>CG7>CG9>CG12>CG2>CG1. The results show that increasing the polymer ratio reduced drug efflux from nanopartilces preparations, which is in accordance with its membrane stabilizing ability [52].

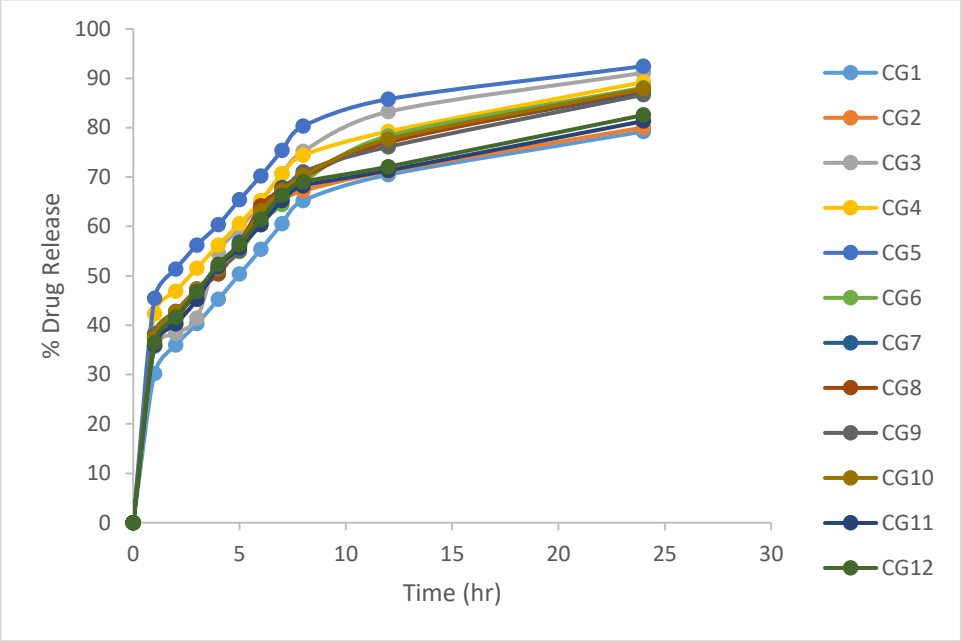

Figure 5: Drug release profile of Gamma Oryganol Loaded Chitosan Nanoparticles

Antioxidant Activity

The findings of the three techniques used to evaluate antioxidant activity are shown in Table 5. The DPPH radical scavenging IC50 values for CG nanoparticles was found to be 57.53± 1.71. The findings of the ABTS test were 1432.06 ± 20.41 µM TEAC/mg DW. Notably, neither the DPPH nor the ABTS assays revealed any discernible change. The CG nanoparticles for FRAP showed significant values of 51.40 ± 3.32 µM TEAC/mg DW. The body of scientific research suggests that the particular test employed for antioxidant capacity of drug.

Table 5: Antioxidant activity of CG nanoparticles by DPPH, ABTS and FRAP methods

Activity	DPPH(%)	IC_{50} (µg/ml)	ABTS (µM TEAC/mg DW)	FRAP (µM TEAC/mg DW)
CG Nanoparticles	57.53±1.71	126.6±1.07	1432.06±20.41	62.50±4.52

The values are shown as mean ± SEM. The means in every column denoted by distinct letters exhibit a significant difference (P<0.05).

Conclusion

The study successfully developed and characterized gamma oryzanol-loaded chitosan nanoparticles with high entrapment efficiency, controlled release, and significant antioxidant activity. The nanoparticulate system demonstrated favorable physicochemical properties, with optimal formulations showing sustained drug release and acceptable PDI for potential pulmonary administration. The DSC and FTIR results suggested strong interaction between the drug and polymer matrix, contributing to the improved stability and performance of the formulation. Moreover, the enhanced antioxidant capacity of the CG nanoparticles indicates their promising role in combating oxidative stress-related disorders. Overall, chitosan nanoparticles present a viable nanocarrier for gamma oryzanol, offering a novel approach for its therapeutic delivery.

Acknowledgments

The authors acknowledge the support of management and the laboratory staff for their assistance during the research work.

Conflict of Interest

The authors declare no conflict of interest.

References

1. Antolovich, M., Prenzler, P. D., Patsalides, E., McDonald, S., & Robards, K. (2002). Methods for testing antioxidant activity. *Analyst*, *127*(1), 183-198.
2. Bairagee, D., Panchawat, S., Jain, N., & Pingali, S. (2024). Controlling the Drug Release Rate and Targeted Drug Delivery to the Desired Site by Molecular Simulation. *Drug Delivery Systems Using Quantum Computing*, 353-387.
3. Bairagee, D., Verma, P., Jain, N., & Jain, N. (2022). Fabrication and in vitro characterization of Niosomal formulations for controlled delivery of ranitidine HCl. *Lat Am J Pharm*, *41*(1), 85-91.
4. Bera, R. K., Pal, T., Ghosh, N., Kundu, A., Ghosh, R., Srivalli, K., & Biswas, K. (2023). Nanomaterials Drug Delivery System in Herbal Formulation For Antidiabetic Activity: A Review. *International Journal*, *10*(5), 955-973.
5. Choudhary, M., Kaur, A., & Kaur, P. (2023). Recent Development in Nanoencapsulation of β-Sitosterol and γ-Oryzanol and Food Fortification. In *Handbook of Nanoencapsulation* (pp. 65-81). CRC Press.
6. Date, A. A., Hanes, J., & Ensign, L. M. (2016). Nanoparticles for oral delivery: design, evaluation and state-of-the-art. *Journal of Controlled Release*, *240*, 504-526.
7. Dewanjee, S., Chakraborty, P., Mukherjee, B., & De Feo, V. (2020). Plant-based antidiabetic nanoformulations: the emerging paradigm for effective therapy. *International journal of molecular sciences*, *21*(6), 2217.
8. Elmowafy, E., El-Derany, M. O., Casettari, L., Soliman, M. E., & El-Gogary, R. I. (2023). Gamma oryzanol loaded into micelle-core/chitosan-shell: from translational nephroprotective potential to emphasis on sirtuin-1 associated machineries. *International Journal of Pharmaceutics*, *631*, 122482.
9. Ghannam, N., Kingston, M., Al-Meshaal, I. A., Tariq, M., Parman, N. S., & Woodhouse, N. (1986). The antidiabetic activity of aloes: preliminary clinical and experimental observations. *Hormone Research in Paediatrics*, *24*(4), 288-294.
10. Jagetia, G. C., & Baliga, M. S. (2004). The evaluation of nitric oxide scavenging activity of certain Indian medicinal plants in vitro: a preliminary study. *Journal of Medicinal Food*, *7*(3), 343-348.
11. Jagetia, G. C., & Lalhmangaihi, C. (2018). Phytochemical profiling and antioxidant activity of Lajwanti Mimosa pudica Linn. in vitro. *Int J Plant Stud*, *1*, 1-13.
12. Khormali, M., & Farahpour, M. R. (2024). The navel nanoethosomal formulation of gamma-oryzanol attenuates testicular ischemia/reperfusion damages. *Heliyon*, *10*(7).
13. Moharram, H. A., & Youssef, M. M. (2014). Methods for determining the antioxidant activity: a review. *Alexandria Journal of Food Science and Technology*, *11*(1), 31-42.
14. Nie, X., Chen, Z., Pang, L., Wang, L., Jiang, H., Chen, Y., ... & Zhang, J. (2020). Oral nano drug delivery systems for the treatment of type 2 diabetes mellitus: an available administration strategy for antidiabetic phytocompounds. *International journal of nanomedicine*, 10215-10240.
15. Panday, S., Patel, V. K., & Shukla, R. K. (2023). NATURAL BIO-POLYMER:-A REWARD ON CHITOSAN LOADED GAMMA ORYZANOL NANOPARTICLES.
16. Paul, R. K., Kesharwani, P., & Raza, K. (2021). Recent update on nano-phytopharmaceuticals in the management of diabetes. *Journal of Biomaterials Science, Polymer Edition*, *32*(15), 2046-2068.
17. Rana, P., & Bala, R. (2024, October). Phyto-nanotechnology for the treatment of diabetes. In *AIP Conference Proceedings* (Vol. 3209, No. 1). AIP Publishing.
18. Rawal, T., Mishra, N., Jha, A., Bhatt, A., Tyagi, R. K., Panchal, S., & Butani, S. (2018). Chitosan nanoparticles of gamma-oryzanol: Formulation, optimization, and in vivo evaluation of anti-hyperlipidemic activity. *Aaps Pharmscitech*, *19*, 1894-1907.
19. Shahidi, F., & Zhong, Y. (2015). Measurement of antioxidant activity. *Journal of functional foods*, *18*, 757-781.
20. Sharif, N., Golmakani, M. T., & Hajjari, M. M. (2022). Integration of physicochemical, molecular dynamics, and in vitro evaluation of electrosprayed γ-oryzanol-loaded gliadin nanoparticles. *Food Chemistry*, *395*, 133589.
21. Tiruwa, R. (2016). A review on nanoparticles-preparation and evaluation parameters. *Indian journal of pharmaceutical and biological research*, *4*(2), 27.
22. Yang, K. M., & Chiang, P. Y. (2019). Preparation and evaluation of release formulation of γ-oryzanol/algae oil self-emulsified with alginate beads. *Marine Drugs*, *17*(3), 156.